*Annual Review of Analytical Chemistry*

# DNA Nanotechnology-Enabled Interfacial Engineering for Biosensor Development

Dekai Ye,[1,2] Xiaolei Zuo,[1,3] and Chunhai Fan[1]

[1]Division of Physical Biology and Bioimaging Center, Shanghai Synchrotron Radiation Facility (SSRF), Shanghai Institute of Applied Physics, Chinese Academy of Sciences, Shanghai 201800, China; email: fchh@sinap.ac.cn

[2]University of Chinese Academy of Sciences, Beijing 100049, China

[3]Institute of Molecular Medicine, Renji Hospital, Schools of Medicine and Chemistry and Chemical Engineering, Shanghai Jiao Tong University, Shanghai 200127, China



Annu. Rev. Anal. Chem. 2018. 11:3.1–3.25

The *Annual Review of Analytical Chemistry* is online at anchem.annualreviews.org

https://doi.org/10.1146/annurev-anchem-061417-010007



## Keywords

interfacial engineering, biosensor, DNA nanotechnology, framework nucleic acid, self-assembly

## Abstract

Biosensors represent biomimetic analytical tools for addressing increasing needs in medical diagnosis, environmental monitoring, security, and biodefense. Nevertheless, widespread real-world applications of biosensors remain challenging due to limitations of performance, including sensitivity, specificity, speed, and reproducibility. In this review, we present a DNA nanotechnology-enabled interfacial engineering approach for improving the performance of biosensors. We first introduce the main challenges of the biosensing interfaces, especially under the context of controlling the DNA interfacial assembly. We then summarize recent progress in DNA nanotechnology and efforts to harness DNA nanostructures to engineer various biological interfaces, with a particular focus on the use of framework nucleic acids. We also discuss the implementation of biosensors to detect physiologically relevant nucleic acids, proteins, small molecules, ions, and other biomarkers. This review highlights promising applications of DNA nanotechnology in interfacial engineering for biosensors and related areas.

## 1. INTRODUCTION

Biosensors have long been expected to be an important driving force in medical diagnosis and treatments, especially with the ever-increasing identification of traceable biomarkers for various diseases (1–4). However, with the exception of glucose meters for diabetes monitoring, there have been few commercial successes and real-world applications of biosensors. Among many possible reasons is that the performance of biosensors remains limited as compared to their natural counterparts in vivo (5). One would envisage the minute-scale rapid capture of single molecule–level biomarkers under a complex biological environment, which nevertheless is far from the ability of existing biosensors (5). To meet these high-end requirements, researchers have exploited various approaches, including molecular biotechnology and nanotechnology, to improve the power of biomolecular interactions in vitro (6–10). In particular, DNA nanotechnology represents a highly programmable approach to engineer the topological structure of biosensing interfaces, which enables better mimicking of natural biointerfaces with a high order of biomolecule organization and biocompatibility (3, 11–19).

In this review, we first introduce basic concepts of biosensing interfaces and their important roles in developing biosensors, with a primary focus on the DNA-based biosensing interface. In Section 2, we describe the motivations and challenges of interfacial engineering for biosensors, as well as the physiochemical perspectives of DNA assembly on the biosensing interface. In Section 3, we provide an overview of recent progress in DNA nanotechnology and its advantages for interfacial engineering. In Section 4, we summarize the main designs of interfacial engineering and their applications in biomolecular detection. In Section 5, we review the applications of DNA nanotechnology-enabled in vivo biosensing.

## 2. FUNDAMENTALS OF BIOSENSING INTERFACES

In a typical biosensor, target-responsive recognition occurs at the interface, where the immobilized probe captures target molecules in bulk solution (**Figure 1*a***). As an example, DNA sensors or DNA microarrays that are useful for quantifying DNA/RNA concentrations and determining gene expression or genotypes generally rely on interfacial DNA hybridization reactions (10, 20). Unlike base pairing in solution, DNA hybridization at the interface is restricted by the accessibility of target DNA molecules to the immobilized DNA probes, which poses a limit on sensitivity, specificity, and speed. Efforts have been made to develop various strategies to reduce the interfacial heterogeneity and to overcome energy barriers to improve thermodynamics and kinetics of DNA hybridization reactions at the biosensing interface (3, 9, 11, 21–28).

Using the assembly of thiolated DNA probes on the gold surface as an example, DNA molecules in solution are spontaneously adsorbed on Au and then reorganized into a self-assembled monolayer (SAM) as a consequence of the specific Au–S interaction (29). To form a stable SAM, its free energy must be lower than the solvent that separated DNA molecules, which is composed of entropy (S) and enthalpy (H) components (10, 24, 25, 30–32). Perhaps as a result of the compensation for the entropy loss during the interfacial assembly, DNA molecules on Au tend to be aggregated or segregated to gain enthalpy. These include electrostatic attraction between DNA phosphate and Au, nucleotides and Au interfaces, and intra- and inter-hydrogen bonding of DNA and phase segregation (29). Hence, the high heterogeneity of DNA immobilization on the surface is a major hurdle in developing high-performance DNA sensors (3, 9, 11, 33). We now understand that the monolayer on Au is far from homogeneous because of the presence of nonspecific adsorption, disordered conformations, and the entanglement and segregation of DNA probes, which greatly reduce the accessibility of these surface-confined DNA probes (**Figure 1*b***). To realize the

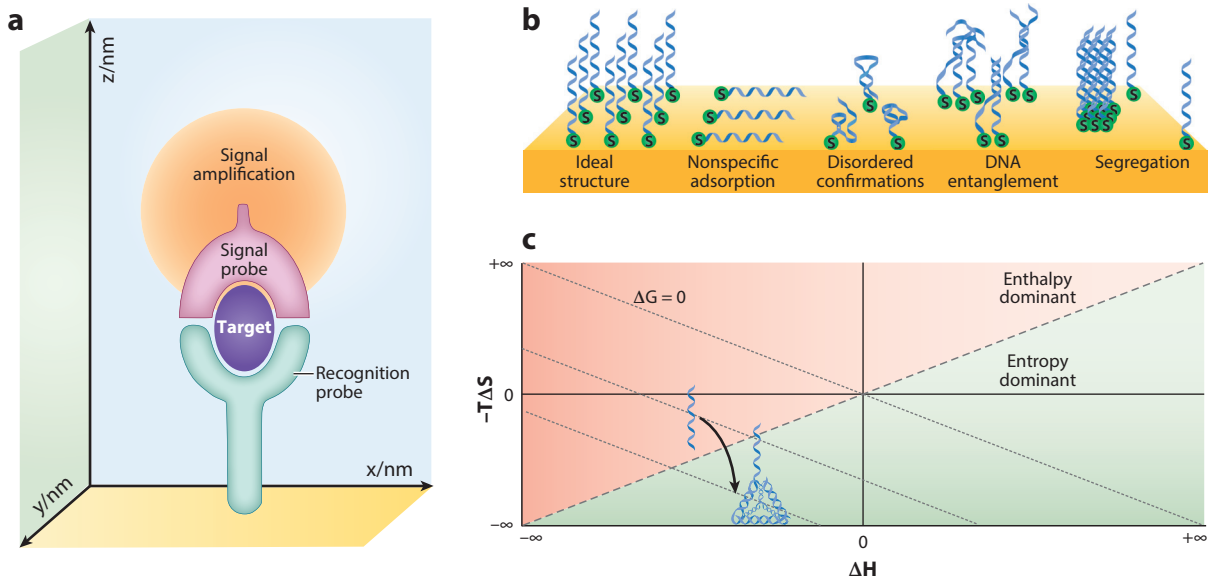


**Figure 1**

Principles of a biosensor and a DNA-based biosensing interface. (*a*) Scheme of a typical biosensor design. Biorecognition probes are immobilized on the biosensing interface and capture target molecules (e.g., DNA, proteins, small molecules, ions) in bulk solution. After target binding, signal probes are used to produce measurable signals, frequently with the help of signal amplification methods. (*b*) A DNA-decorated gold surface for biosensors. The heterogeneity of the interface is due to the presence of nonspecific adsorption, disordered conformations, entanglement, and segregation of DNA probes, which preclude the formation of an ideal self-assembled monolayer. Modified with permission from Reference 29. Copyright 2014, American Chemical Society. (*c*) Thermodynamic consideration for interfacial engineering. An enthalpy–entropy compensation strategy by preforming ordered DNA nanostructures might increase the interfacial homogeneity. Modified with permission from Reference 35. Copyright 2015, Nature Publishing Group.

near-ideal DNA assembly on Au, one might consider exploiting enthalpy–entropy compensation by preforming ordered DNA nanostructures to reduce interfacial aggregation or segregation (34, 35) (**Figure 1*c***).

## 3. PRINCIPLES OF DNA NANOTECHNOLOGY

DNA is the primary genetic material with the well-known double helix structure. In the early 1980s, Jones et al. (36) first proposed that DNA could be used a construction material for making well-defined nanostructures by self-assembling in a one-pot mixture of oligonucleotides with designed sequences. We have witnessed exponential growth in the degree of sophistication of DNA nanostructures over the past two decades (15, 36–63) (**Figure 2**). The success of DNA nanotechnology comes partially from the nearly quantitative understanding of DNA thermodynamics, allowing precise prediction of the folded state of single-stranded DNA (ssDNA) and their interactions with other ssDNA. Today, with the rapid advances in chemical synthesis of oligonucleotides, researchers can construct DNA libraries with rational design and programmably assemble DNA nanostructures using Watson-Crick base-pairing rules in a bottom-up manner. Scaffolds of basic platonic solids, two-dimensional (2D) single-layer sheets, three-dimensional (3D) DNA lattices, and containers and nanostructures with arbitrary curvature have been reported (40, 56, 58, 59, 64–67) (**Figure 2*a–e***). Beyond the static DNA nanostructures, dynamic DNA nanotechnology

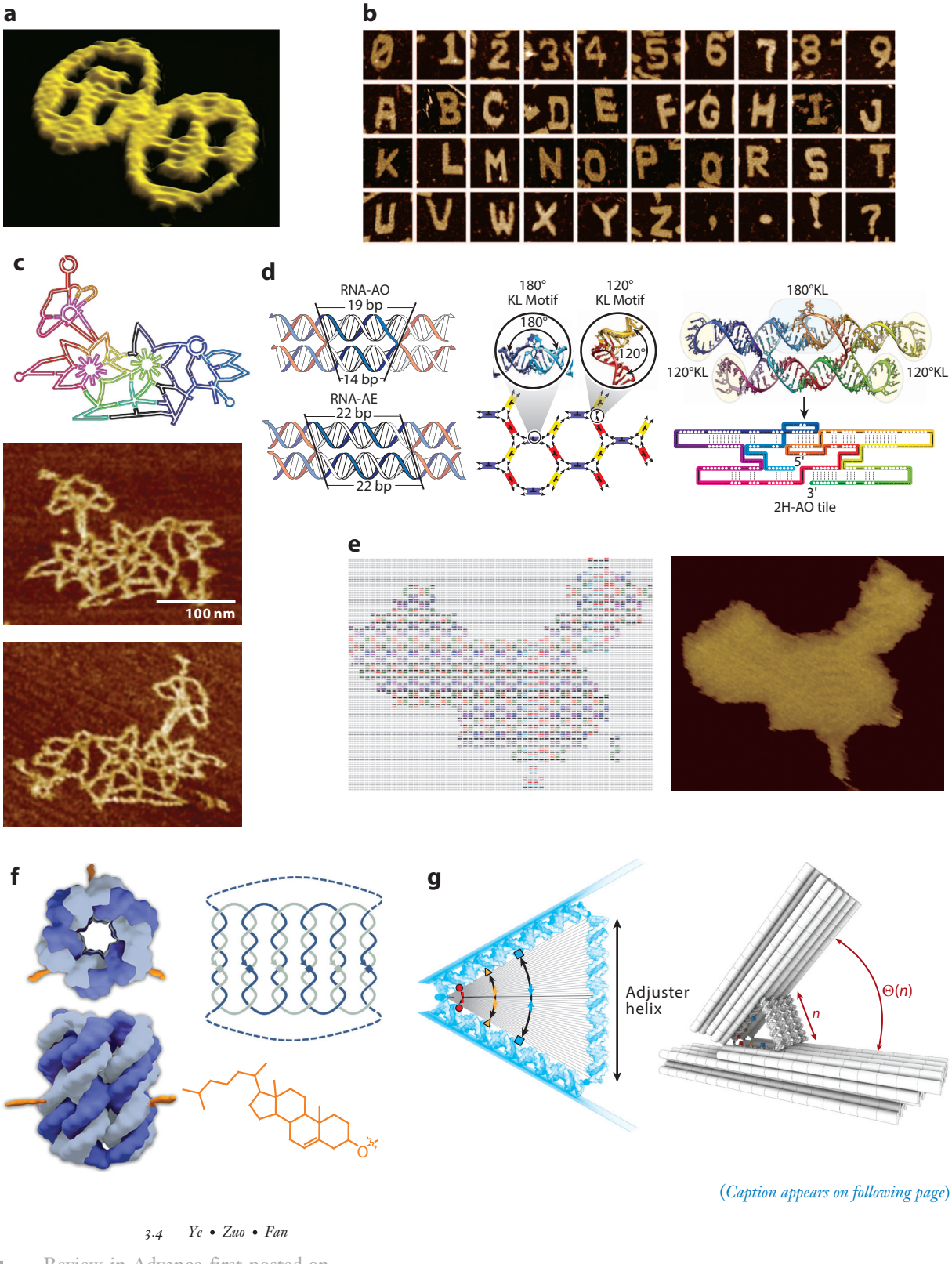


(Caption appears on following page)

**Figure 2** (*Figure appears on preceding page*)

Representative examples of structural DNA nanotechnology. (*a*) Smiley-face DNA origami nanostructure. Modified with permission from Reference 65. Copyright 2017, Nature Publishing Group. (*b*) AFM images of complex shapes designed using a single-stranded tile. Modified with permission from Reference 58. Copyright 2012, Nature Publishing Group. (*c*) Representative design and AFM images of intricate two-dimensional flower-and-bird nanopatterns. Modified with permission from Reference 55. Copyright 2015, Nature Publishing Group. (*d*) ssRNA for tile assembly. Modified with permission from Reference 74. Copyright 2014, AAAS. (*e*) The design (*left*) and AFM image (*right*) of a highly asymmetric DNA origami map of China. Modified with permission from Reference 66. Copyright 2006, Science China Press Co., Ltd. (*f*) Biomimetic channels for transport of charged molecular cargo. Modified with permission from Reference 72. Copyright 2016, Nature Publishing Group. (*g*) High-resolution DNA positioning device for placing molecules with Bohr radius resolution. Modified with permission from Reference 50. Copyright 2015, Nature Publishing Group. Abbreviations: AFM, atomic force microscopy; KL, kissing loop; ssRNA, single-stranded RNA.



combines DNA nanotechnology with responsive aptamers, DNAzyme catalysis, or DNA strand displacement reactions to create dynamic DNA nanostructures with motions and functions (49, 50, 68–70). Prototypes of dynamic DNA nanotechnology can be traced to strand displacement reaction–based hybridization chain reaction and molecular machines. The simplicity of strand displacement reaction enables broad applications in driving many types of dynamic DNA nanostructures, including molecular motors, walkers, molecular circuits, and catalytic amplifiers (47, 60), and the method holds great potential for various biological applications. Another elegant example lies in the recreation of the functional principle of biological ion channels (71, 72). Howorka and colleagues (72) employed DNA assembly to create atomistically determined molecular valves to control cargo transportation (**Figure 2*f***). Funke & Dietz (50) designed a molecular positioning device made of two pieces of DNA origami with a tunable angle, which achieved the smallest displacement step reported of 0.04 nm, i.e., even smaller than the Bohr radius (**Figure 2*g***). In addition to DNA, RNA nanostructures (73, 74) have attracted much recent interest because they are more adaptable for in vivo folding (**Figure 2*d***).

DNA nanotechnology holds remarkable potential for engineering biosensing interfaces for several reasons (3). First, the programmable assembly of ordered DNA nanostructures with well-defined hydrogen bonds provides a powerful means to realize the entropy–enthalpy compensation. The diverse shapes and dimensions of DNA nanostructures and their versatile yet controllable chemical modifications also offer high flexibility. Second, this high degree of assembly control enables the creation of DNA nanostructure modules that have predictable physical and chemical properties for realizing important functions. Third, the use of these DNA modules to assemble hybrid or multicomponent structures allows for the rational design of multicomponent and multilength-scale interfaces.

One type of particularly interesting DNA/RNA nanostructure is framework nucleic acids (FNAs; **Figure 3**). Here, we refer to FNAs in self-assembled DNA structures with surrounding DNA strands and well-defined cavities (11, 56, 57, 59, 73, 75, 76). Naturally existing FNAs include telomere G-quadruplex, riboswitches, and ribozymes, whereas artificial FNAs include aptamers, DNAzymes, and various DNA/RNA nanostructures. DNA polyhedra are a type of typical FNA that can be readily fabricated using either tile or origami assembly (**Figure 3*a–d***). In contrast to linear DNA/RNA, information is stored in the 2D/3D spatial conformation rather than the 1D sequence (although the conformation is dependent on the sequence). Perhaps more importantly, a number of ions, small molecules, biomacromolecules, and inorganic nanoparticles can be incorporated into the cavities, which add a functional dimension to FNAs. Moreover, FNAs serve as a discrete scaffold for site-specific chemical/biochemical functionalization of small molecules, proteins, and nanoparticles either at the edges or in the cavity, which endows

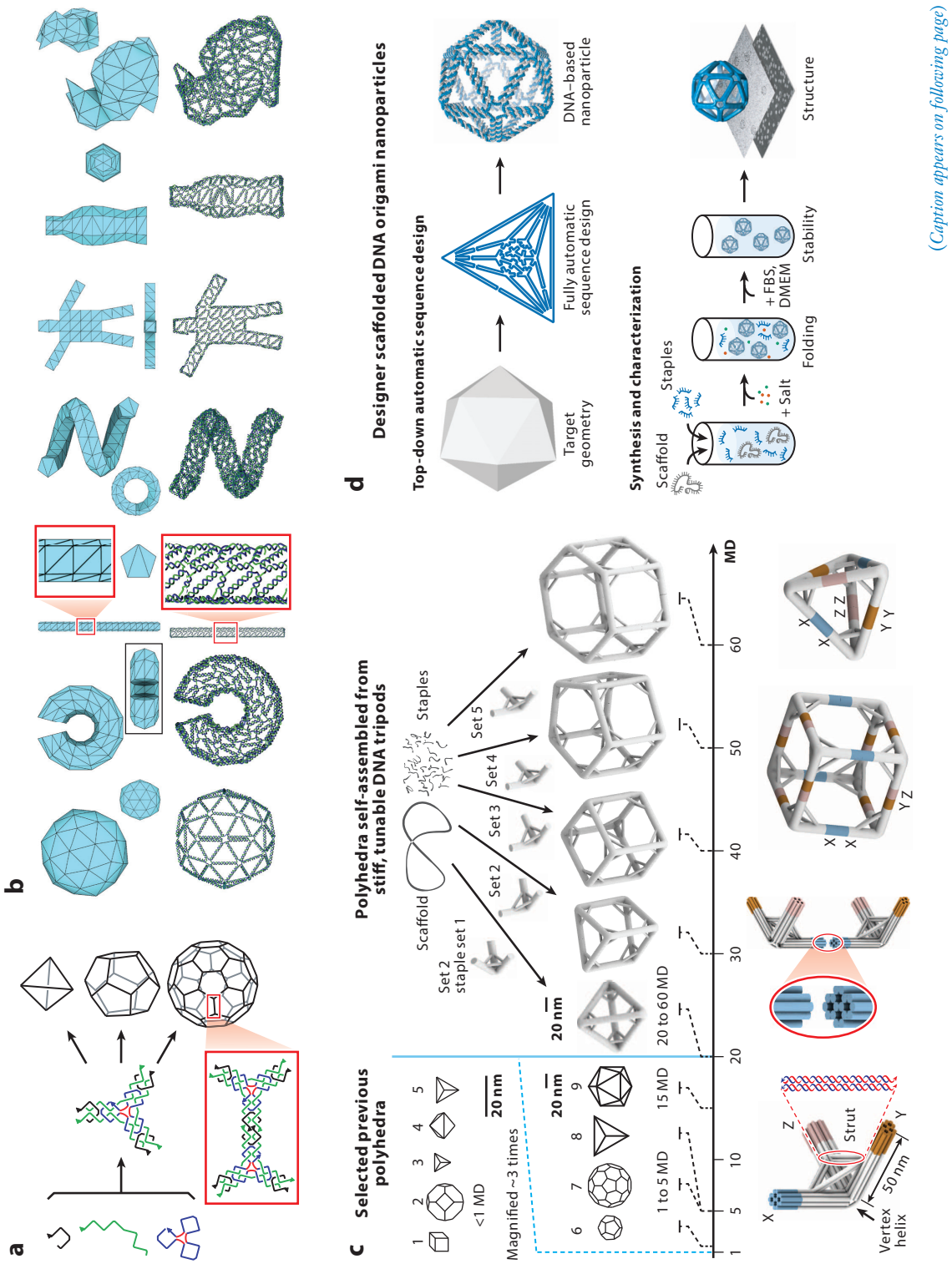


(Caption appears on following page)

**Figure 3** (*Figure appears on preceding page*)

Framework nucleic acids. (*a*) Self-assembly of three-point-star motifs and a polyhedral in a one-pot process from DNA single strands. Modified with permission from Reference 57. Copyright 2008, Nature Publishing Group. (*b*) Folding of arbitrary polygonal digital meshes. Modified with permission from Reference 56. Copyright 2015, Nature Publishing Group. (*c*) A DNA origami polyhedral self-assembled from DNA tripods. Modified with permission from Reference 59. Copyright 2014, AAAS. (*d*) The fully automatic sequence design was used for DNA nanostructures. A polymerase chain reaction was used to synthesize DNA nanostructures, and cryo-electron microscopy was used to characterize the DNA nanostructures. Modified with permission from Reference 15. Copyright 2016, AAAS. Abbreviations: DMEM, Dulbecco's modified Eagle's medium; FBS, fetal bovine serum.

FNAs with versatile functions. Given these advantages, FNAs have been actively explored for engineering various biointerfaces that are discussed in the following sections.



## 4. ENGINEERING OF BIOSENSING INTERFACES

Theoretical models have predicted that large lateral spacing and upright orientation of immobilized DNA probes favor efficient DNA hybridization at the interface (77, 78). However, it is challenging to reproducibly assemble DNA monolayers with both of these properties (26). The control of the probe density and orientation often represents a trade-off: Lower probe density increases the lateral spacing between DNA probes, whereas DNA probes tend to lie flat on the surface due to the presence of vacancy. Indeed, repulsion between negatively charged DNA probes forms the collective extension forces that extend DNA probes away from the surface in densely packed films (26). Experimental evidence has shown that the DNA probes take flat conformations due to the nonspecific adsorption when the spacing between DNA probes is comparable to their length (79, 80).

### 4.1. Small Molecule–Assisted Interfacial Engineering

DNA probes tend to nonspecifically adsorb to Au surfaces through their bases, which suppress efficient hybridization at the interface (81, 82). Small molecule–assisted interfacial engineering was used to orient the DNA probe perpendicularly and to improve its hybridization ability by displacing the nonspecific adsorption of DNA bases with small molecules, such as 6-mercaptohexanol (MCH), dithiothreitol (DTT), and 3-mercaptopropionic acid (MPA) (79, 83) (**Figure 4*a***).

Tarlov's group and several others provided direct evidence that the displacement of nonspecifically adsorbed DNA bases favors the optimal orientation of immobilized DNA probes (79). X-ray photoelectron spectroscopy revealed that the nitrogen-containing purine and pyrimidine bases of DNA could adsorb on Au with high affinity, despite the major role of thiol–Au interactions (81). Thickness measurements using ellipsometry also revealed that DNA probes were not oriented perpendicular to the surface (79). Furthermore, the hybridization activity can almost be inhibited at high DNA density due to the steric and electrostatic factors. To facilitate interfacial hybridization, two-component monolayers consisting of thiol–DNA and a spacer-thiolated molecule (MCH) were developed to minimize the nonspecific adsorption of DNA and Au. Neutron reflectivity analysis showed that DNA strands extended further into solution at such an engineered interface (80). Arinaga et al. (84) demonstrated that the conformational change of the DNA layer was predominantly of electrostatic origin. The surface charge can be altered by coimmobilizing small molecules and controlling the electrode bias potential. Hamad-Schifferli and coworkers (85) studied key parameters, including MCH concentration and reaction time, to achieve optimized DNA conformations on Au. O'Sullivan and colleagues (86) reported that the optimal hybridization efficiency for 100 nM of target DNA was realized at a DNA/MCH ratio of 1:100.

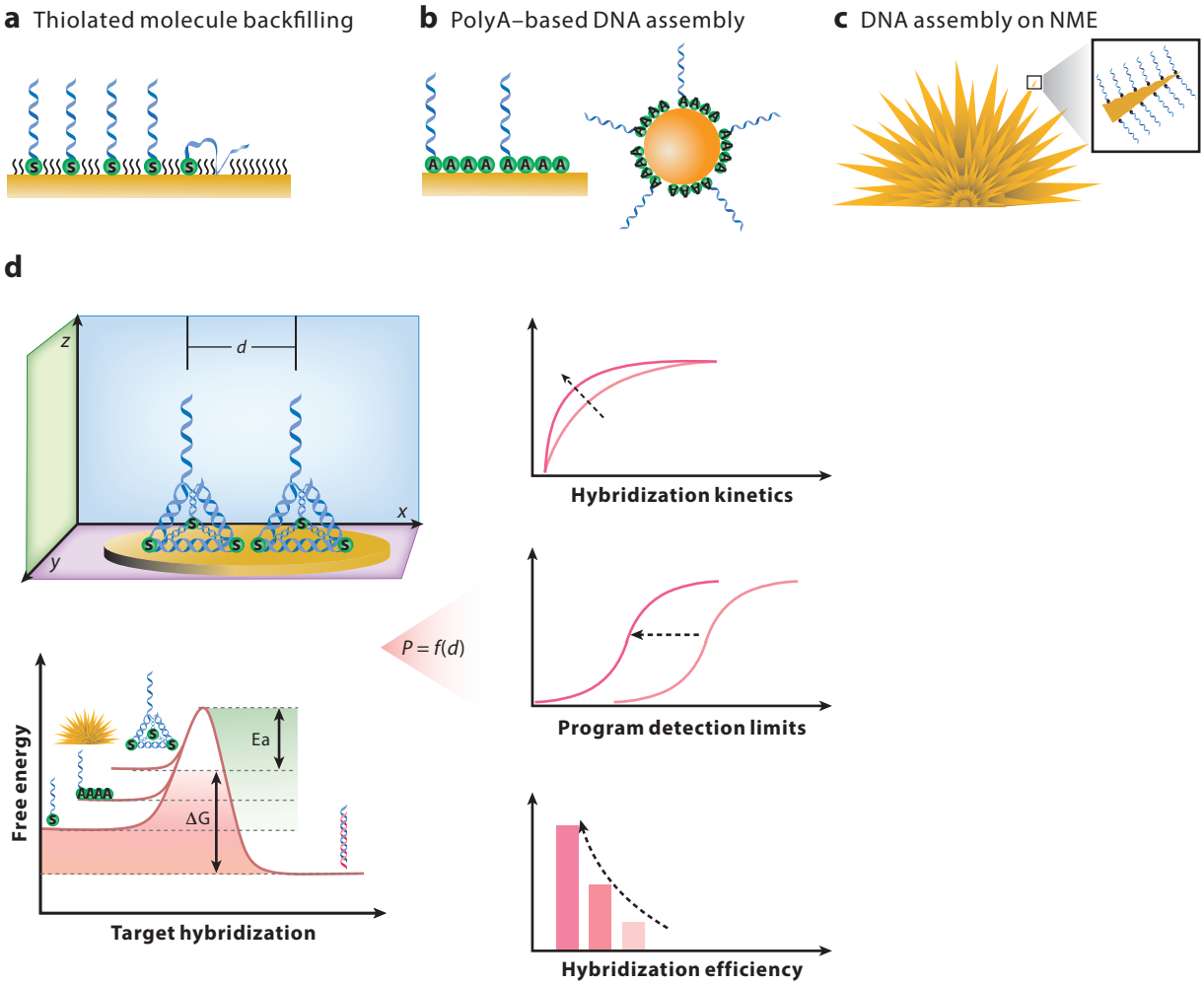


**Figure 4**

Interface engineering strategies. (*a*) Thiolated small molecules are usually used to minimize the nonspecific adsorption between the immobilized DNA probes and solid interface. Modified with permission from Reference 79. Copyright 1997, American Chemical Society. (*b*) Polyadenine (polyA) is used as a substitute of thiol moiety of DNA probes to control the grafting density on the macroscopic solid interface and nanoscale interface. The length of polyA can be programmed to control the lateral distance between DNA probes. Modified with permission from Reference 99. Copyright 2012, American Chemical Society. (*c*) Nanostructured microelectrodes (NMEs) are used to suppress DNA probe aggregation between adjacent probes. Modified with permission from Reference 107. Copyright 2011, American Chemical Society. (*d*) Framework nucleic acids are used for programmable control of the DNA density at the nanoscale. Modified with permission from Reference 11. Copyright 2015, Wiley-VCH.

The small molecule–assisted interfacial engineering strategy has been widely employed to improve the hybridization efficiency, detection limit, and detection selectivity of DNA sensors. For example, Lu and coworkers (87) reported that the use of DNA probe/MCH mixing on the SAM increased the surface hybridization efficiency by 85%. The DNA detection sensitivity could be improved to 50 fM by reducing the surface density of DNA probes from $1.2 \times 10^{13}$ to $1.2 \times 10^{12}$ molecules/cm$^2$ (88). The SAM of MCH can also be used as a layer for protein anchoring after the activation of surface OH groups by epichlorohydrin. Using this method, Sezginturk's

group (89) immobilized a specific antibody to calretinin on an MCH SAM to detect calretinin with the detection limit of 0.11 ng/mL. Artificial serum samples spiked with calretinin were successfully detected.

The use of MCH and thiolated ssDNA to form binary SAMs has proven quite useful for improving biosensing performance. However, this type of SAM does not show high protein resistance. Oligo(ethylene glycol)-terminated thiols are well known to be protein resistant, which has helped them coassemble with thiolated ssDNA. This could improve the detection sensitivity to the picomolar level even in complicated biological fluids such as human serum (90). This method was employed to detect polymerase chain reaction (PCR) amplicons from the genomic DNA of *Escherichia coli* K12, and as little as 60 fg of DNA (equivalent to 10 copies) can be detected. Short thiolated oligonucleotides (e.g., thymines) were also used to form antifouling SAMs as diluents. The background signal changed only 5%, which is approximately seven-fold lower than that of MCH-based SAMs, when the sensor was introduced in a nontarget protein–containing solution (27). The negative charges of the phosphate backbone may prevent nonspecific adsorption in complex samples. To further improve the detection performance, Wang and coworkers (91) developed ternary SAM assembly to improve the signal-to-noise ratio and detection sensitivity. This method addressed the incomplete backfilling and surface defects in the binary SAM, allowing higher resistance to nonspecific adsorption of nucleic acids and proteins. The ternary SAM was also employed in TNT detection by coassembling peptamer, DTT, and MCH (92). The 0.15 pM of TNT can be sensitively detected with a 1,000-fold improvement of sensitivity as compared to binary SAMs. Dharuman et al. (93) used both long-chain [11-mercaptoundecanoic acid (MUDA) and 11-mercaptoundecanol] and short-chain (MCH and MPA) acids to optimize the ternary SAM. They found that the ssDNA/MCH/MUDA ternary SAM exhibited the highest sensitivity. The presence of hydrogen bonds between the −OH group and −COOH head groups was necessary to enhance the electrostatic blockade and form a compact SAM.

## 4.2. Polyadenine-Mediated Interfacial Engineering

Studies on DNA base–Au interactions revealed that the binding affinity of DNA bases on Au follows the order of A>C≥G>T (94–96). In particular, polyA oligonucleotides adsorb strongly on the Au surface, which compares favorably with the well-known Au–S bonding (**Figure 4*b***). The presence of an Au surface can even denature the duplexes of polyA and polyT. The remarkably strong binding affinity of polyA on Au has practical applications for designing thiol-free DNA immobilization strategies (12).

In order to independently control the conformation and grafting density of DNA, polyA nucleotides were used as both an anchoring group and a density control module (26, 97). The tunable length of polyA provides density control: The density decreases as the length of polyA increases. In addition, polyA preferentially binds to Au and blocks other possible adsorption sites, which strongly prevents nonspecific adsorption. This strategy was used to assemble polyA-tailed 15-nucleotide DNA probes on the Au surface (97). Quantitative analysis of immobilization indicated the preferential binding of polyA on Au and the upright conformation of probe portion. The preferential binding of polyA on Au can also be used to detect non-nucleic acid targets such as DNA methyltransferase. Ai and coworkers (98) developed a novel electrochemical method to detect DNA methyltransferase. In the presence of DNA methyltransferase, the designed hairpin probes were methylated and then cleaved into two parts by endonuclease Dpn I, releasing the polyA-tailed products with a methylene blue label. The strong binding affinity of the polyA-tailed products adsorbed on the Au surface and produced a signal for the quantification of DNA methyltransferase.

The polyA-mediated interfacial engineering can be extended to the nanoscopic range for preparing DNA-conjugated Au nanoparticles (AuNPs). The preparation of Au–S chemistry-based

DNA–AuNP nanoconjugates requires the modification of DNA and lacks the density and conformation control of tethered DNA. Recently, to circumvent this problem, a new strategy was developed to immobilize DNA probes via the strong interactions between polyA and Au (99, 100). By regulating the length of polyA, Pei et al. (99) could readily regulate the lateral distance and density of tethered DNA on AuNPs. DNA–AuNPs conjugates with polyA anchoring exhibited significantly faster DNA hybridization kinetics, indicating the proper conformation of DNA on AuNPs. The property of multipoint anchoring of polyA on AuNPs minimizes nonspecific interactions between other bases and Au, eliminating the use of diluent molecules or short DNA sequences employed in a traditional assembly strategy. The conformational change of polyA-tailed DNA on AuNPs was simulated through the finite-difference time-domain method, indicating that longer polyA tails provided a stronger repulsion force for the DNA probe to adopt an upright conformation (101). The polyA-based anchoring method was also used to improve the DNAzyme assembly on AuNPs (102). By tuning the length of polyA, the activity of DNAzymes can be programmed to be regulated, resulting in the maximum 75-fold enhancement in binding affinity. The polyA and hairpin diblocks (DHPs) were designed to amplify the DNA detection signal to achieve 0.01 pM of DNA detection (103). DNA targets triggered the catalytic assembly of DHP1, DHP2, and DHP3 to form numerous polyA-tailed branched DNA junctions. Coupled to AuNP-based colorimetric detection, the polyA-tailed branched DNA junctions brought the AuNPs into close proximity via the assembly of polyA–AuNP, which resulted in remarkable color change. The target DNA can be quantitatively detected.

The strategy of polyA-mediated interfacial engineering can be generalized to the functionalization of nanocarbons, transition-metal dichalcogenides, metal oxides, and several other nanoparticles (104, 105). For example, polycytosine (polyC) DNA has high affinity for the interface engineering of silver nanoparticles (AgNPs). The intrinsic Ag–cytosine (Ag–C) coordination allows for the assembly of DNA–AgNP conjugates. These DNA–AgNPs showed favorable stability at high ionic strength (300 mM of NaCl) and high temperature (up to 90°C). Compared to thiolated DNA-modified AgNPs, the polyC-mediated DNA–AgNP assembly possessed more efficient molecular recognition capability and faster hybridization kinetics (4.5-fold improvement in rate constant) (104). Lu et al. (105) systematically investigated the assembly of polyC DNA on $MoS_2$, $WS_2$, and $Fe_3O_4$ nanoparticles, providing a simple solution for functionalizing nanomaterials with polyC DNA. Thus, the use of polyA or polyC to engineer the biosensing interface provides a simple solution for biosensor development.

### 4.3. Inorganic Nanostructure–Supported Interfacial Engineering

Nanostructured interfaces provide a direct means to improve the accessibility of immobilized biomolecular probes by altering mass transfer at the interface (**Figure 4*c***). Kelley and coworkers (1, 2, 4, 5, 7, 9, 21, 33, 106–116) developed nanostructured microelectrodes (NMEs) that could be employed to investigate biosensing sensitivity as a function of degree of nanostructuring states. NMEs were prepared via electrodeposition on silicon wafers, which were then assembled with thiolated DNA probes (9). Importantly, the nanostructuring states could be finely tuned with electrodeposition time and plating potential. All-atom molecular dynamics simulation revealed that high curvature structures of NMEs suppress DNA probe aggregation between adjacent probes and increase interfacial mass transfer, resulting in high accessibility of immobilized DNA strands (21). The detection limit of NME-based sensors for DNA/RNA reached 10 aM, which represents a 10,000-fold improvement as compared to that with macroelectrodes (9).

The ultrahigh sensitivity of NME-based sensors presents many opportunities. For example, bacterial RNA can be detected within 30 min using NMEs (111). This detection platform can be generalized to analyze a spectrum of clinically relevant analytes, including antibiotic resistance

markers and cancer biomarkers (7). One remarkable example is the use of chip-based NME sensors for rapid analysis of tissue levels of preimplantation mRNA markers, which is related to the development of primary graft dysfunction in recipients after transplant (116). The results can be obtained within 20 min (versus 5 h for quantitative PCR), and small differences in interleukin (IL)-6, IL-10, and adenosine 5′-triphosphate (ATP)11B mRNA can be quantified in a donor's lung biopsy. More recently, to detect cell-free nucleic acids without prior enzymatic amplifications, an electrochemical clamp assay was demonstrated to identify the mutations within 15 min (113). In this strategy, researchers used a collection of oligonucleotides that could sequester closely related sequences in solution to prevent the interference, allowing only the mutated sequence to bind to the probe. The sensor was able to detect 1 fg/μL of A549 exosomal RNA. The accuracy of this NME-based detection is comparable with that of PCR, with the added advantage that it is faster and can be used directly in unpurified serum.



## 4.4. DNA Nanostructure-Guided Interfacial Engineering

DNA nanostructures can precisely control the anchoring of functional molecules and nanoparticles in a site-specific manner (39, 42, 45, 71, 117–123) (**Figures 4*d*, 5**). For example, DNA or aptamers can be site-specifically positioned on DNA origami as extensions of staple stands. Yan's group (124) first demonstrated the linear S-shaped and face-shaped arrangement of proteins by programming the positioning of protein-specific ligands (e.g., aptamers) on DNA origami. Enzyme cascade pairs can also be precisely positioned on DNA origami (**Figure 5*d***), through which the distance-dependent cascade activity can be systematically investigated (23, 125). Wilner et al. (126) first demonstrated the use of a hexagon-shaped DNA framework for the topological arrangement of enzyme cascade pairs, leading to the activation of an enzyme cascade (**Figure 5*e***). Yan and coworkers (22) encapsulated enzymes in a DNA nanocage with well-controlled stoichiometry and architecture. The impact of encapsulation and proximal polyanionic surface increased the substrate turnover rate of the enzymes (**Figure 5*d***). Our group (127) demonstrated that rectangular DNA origami could be folded into tubular DNA origami to constrain the space of enzyme cascade reaction and enhance the reaction activity. Beyond the static arrangement of proteins, reversible conjugation of proteins can be achieved through toehold-mediated stand-displacement reaction. Similarly, AuNPs (128, 129) and nanorods (130) were selectively placed on the rectangular DNA origami with nanometer accuracy to form "hot spots" of enhanced electromagnetic field between nanoparticles.

DNA origami nanostructures have been employed as soluble nanoscale chips for nucleic acid detection. Ke et al. (13) anchored pairs of 20-base ssDNA probes on rectangular DNA origami to detect complementary DNA/RNA (**Figure 5*b***). Hybridization to their targets in solution was readily visualized using atomic force microscopy (AFM), which could quantify binding events in a label-free manner. We developed a map-based origami chip for single nucleotide polymorphism (SNP) typing (67) (**Figure 5*c***). The spatial addressability of an asymmetric map obviated the use of index oligonucleotides and supported multiplexing detection of SNPs. In addition, a direct visual readout of the target sequence was developed to visualize the SNP by combining kinetic methods with AFM imaging (131) (**Figure 5*a***).

## 4.5. Framework Nucleic Acid–Based Interfacial Engineering

The hollow structure of FNAs maximizes their spatial occupation with minimal use of DNA materials, which are ideal for assembling higher-order DNA architectures at the interface (132–135). Although inorganic nanostructures can be created on a macroscopic interface by either surface etching or deposition of metal nanoparticles, reproducible preparations of such

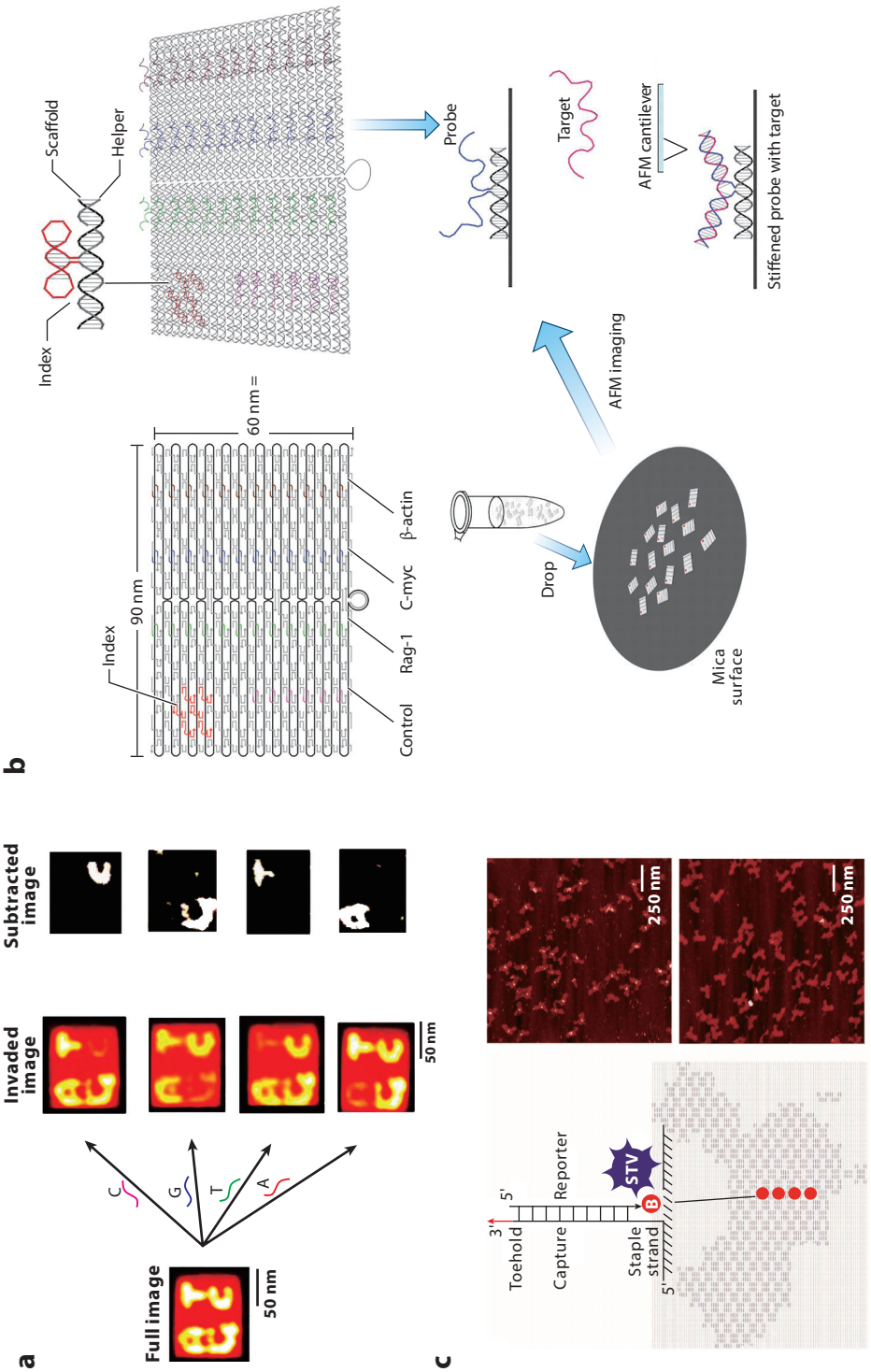

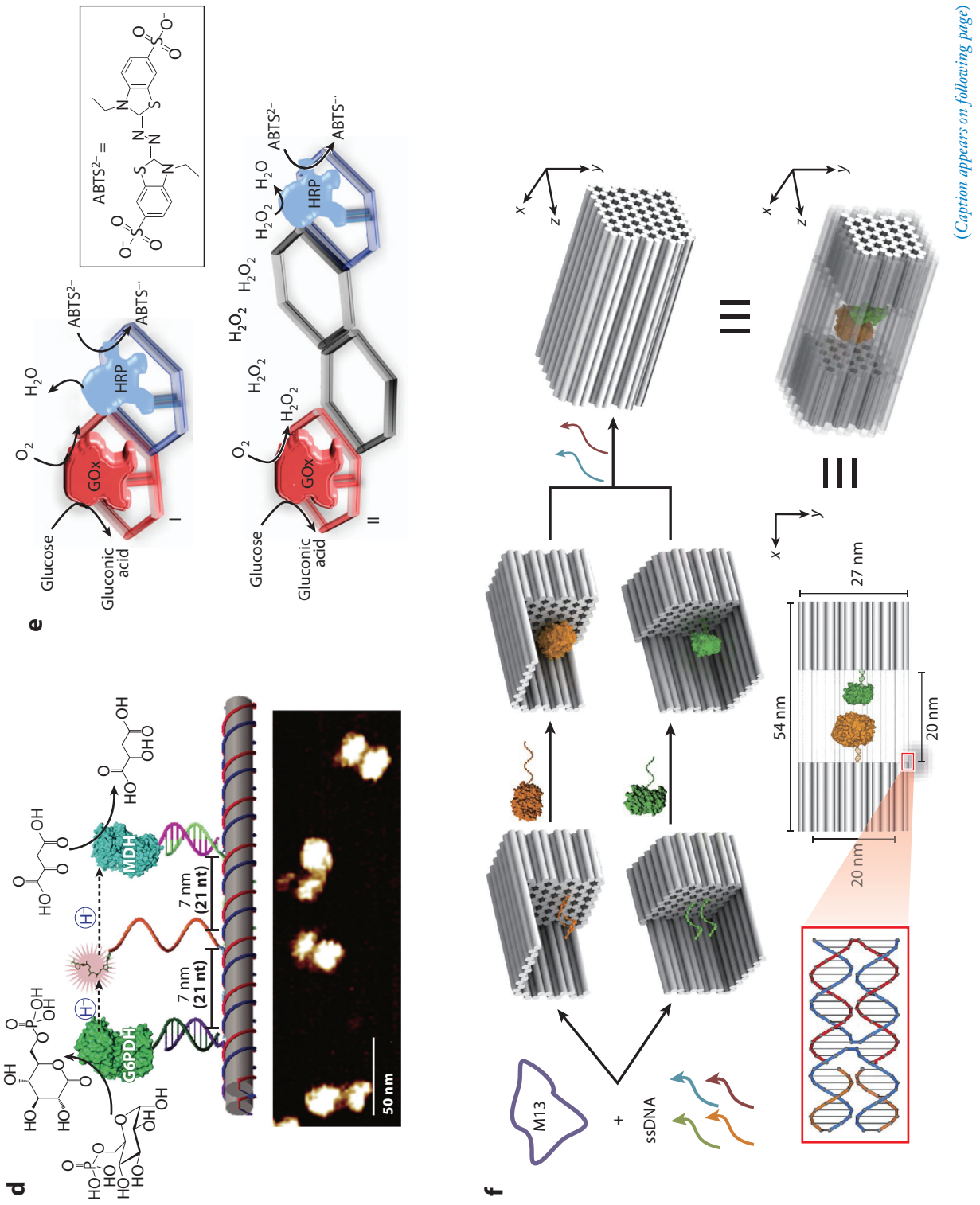


*(Caption appears on following page)*

**Figure 5** (*Figure appears on preceding page*)

(*a*) Direct visual detection of SNPs using DNA origami nanochips. Modified with permission from Reference 131. Copyright 2011, American Chemical Society. (*b*) Visualized detection of multiple targets (control, Rag-1, C-myc, and β-actin) using DNA tiles. Modified with permission from Reference 13. Copyright 2008, AAAS. (*c*) The principle of toehold-mediated strand displacement reaction on the China map–shaped DNA (*left*) origami and AFM images for DNA origami before and after strand-displacement reaction (*right*). Modified with permission from Reference 67. Copyright 2010, Wiley-VCH. (*d*) The $NAD^+$-modified swinging arm was arranged between two dehydrogenases to facilitate enzyme cascade reaction. Modified with permission from Reference 23. Copyright 2014, Nature Publishing Group. (*e*) Programmable arrangement of HRP and GOx enzymes on two-hexagon and four-hexagon strips. Modified with permission from Reference 126. Copyright 2009, Nature Publishing Group. (*f*) Enzyme cascade pairs were encapsulated in a DNA nanocage. Modified with permission from Reference 22 under the terms of the Creative Commons Attribution 4.0 International License, **http://creativecommons.org/licenses/by/4.0**. Abbreviations: A, adenine; ABTS, 2,2′-Azino-bis (3-ethylbenzothiazoline-6-sulfonic acid); AFM, atomic force microscopy; C, cytosine; G, guanine; G6PDH, glucose-6-phosphate dehydrogenase; GOx, glucose oxidase; HRP, horseradish peroxidase; MDH, malic dehydrogenase; SNP, single nucleotide polymorphism; ssDNA, single-stranded DNA; STV, streptavidin; T, thymine.



nanostructured surfaces remain technically challenging (11). Photolithography provides a potential solution for the preparation of nanostructures, but it is hampered by its high cost and the difficulty in making 2D/3D structures with 10-nm–scale resolution. In this regard, FNAs can provide high-resolution nanostructured interfaces with relatively low cost and high reproducibility (3, 29).

The secondary structures of DNA, including hairpin, pseudoknot, and quadruplex, can be used as building blocks to engineer the biosensing interface, which may help avoid interstrand entanglement due to the increased rigidity (6, 28, 136–140). Fan, Plaxco, and Heeger (6) first developed an electrochemical DNA sensor by immobilizing ferrocene-labeled DNA stem-loop probes on Au electrodes (**Figure 6*a***). DNA hybridization at the interface induces a large conformational change in the immobilized hairpin probes, which significantly alters the electron transfer distance and leads to measurable electrochemical signals. As little as 10 pM of target DNA can be detected when using ferrocene labels. The detection sensitivity can be improved down to 10 fM via signal amplification using horseradish peroxidase (HRP) (134) (**Figure 6*a***). The superiority of 2D probes over single-stranded ones ensures better orientation and less interprobe entanglement at the interface. Based on this principle, various types of DNA sensors were developed using pseudoknot, triple-stem, and partially hybridized probes, which exhibit high specificity and selectivity for direct use in blood serum. This principle has also been generalized to detect other types of molecular targets, including proteins, small molecules, and metal ions, by changing 2D DNA probes to structured aptamers or DNAzymes (138).

The use of 2D DNA structures increases the order of the biosensing interface; however, the limited rigidity of the 2D structure leads to an inherent reproducibility problem, especially at a high probe density that perturbs the formation of 2D structures. Three-dimensional FNAs, especially polyhedra, are potentially highly rigid structures that may circumvent this problem (141). Pei et al. (75) developed a tetrahedral DNA nanostructure (TDN)-based platform for biosensor development (**Figure 6*b***). To design such a biosensing interface, a TDN was appended with a DNA recognition probe at one vertex and three thiols on the other vertices. The three thiols formed strong Au–S bonds on gold, which served as a three-point attachment for anchoring the DNA tetrahedron. The DNA recognition probe could be well oriented at the top vertex. This TDN structure led to a stable and reasonably homogeneous DNA recognition layer with improved recognition capability. The sensitivity of the TDN-based biosensing interface was enhanced by a factor of 250 as compared to that using ssDNA probes. This TDN-based electrochemical DNA sensor also exhibited high specificity that could differentiate single-base mutations by approximately 100-fold on TDNs.

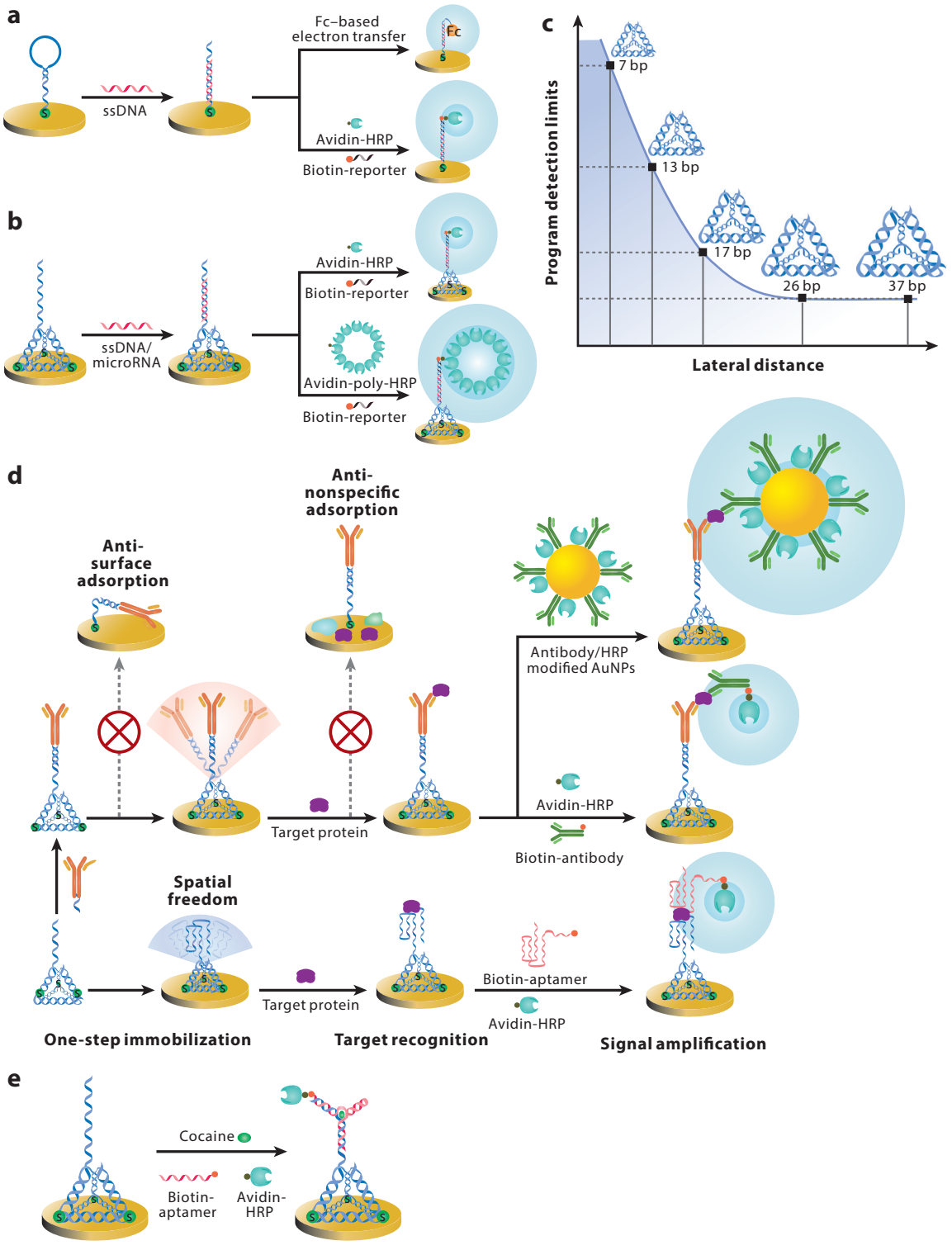


(Caption appears on following page)

**Figure 6** (*Figure appears on preceding page*)

DNA detection using framework nucleic acid–based probes. (*a*) Two-dimensional stem-loop structures for the construction of DNA biosensors. Either Fc or enzyme (e.g., HRP) can be used to produce a measurable signal. (*Top*) Modified with permission from Reference 6. Copyright 2003, National Academy of Sciences. (*Bottom*) Modified with permission from Reference 134. Copyright 2008, American Chemical Society. (*b*) Three-dimensional TDNs for the construction of DNA biosensors. HRP or poly-HRP can be used for signal amplification. (*Top*) Modified with permission from Reference 75. Copyright 2010, Wiley-VCH. (*Bottom*) Modified with permission from Reference 135. Copyright 2012, Nature Publishing Group. (*c*) The size of TDNs can program the lateral distance and detection limit of DNA biosensors. (*d*) Protein detection using TDNs. Antibodies or aptamers can be conjugated on TDNs and used as recognition probe for protein detection. (*Top*) Modified with permission from Reference 75. Copyright 2010, Wiley-VCH Verlag. (*Bottom*) Modified with permission from Reference 132. Copyright 2014, American Chemical Society. (*e*) TDN-based biosensing design for small molecules. Modified with permission from Reference 133. Copyright 2011, American Chemical Society. Abbreviations: AuNP, gold nanoparticle; Fc, ferrocene; HRP, horseradish peroxidase; ssDNA, single-stranded DNA; TDN, tetrahedral DNA nanostructure.



In addition to the homogeneity, the ability to program the size of the TDNs is another important feature of the 3D TDN-based biosensing interface (**Figure 6*c***). By simply changing the size of TDNs, the lateral distance between DNA probes can be programmed (11). For example, the lateral distance changes from 2.4 nm to 12.6 nm when the edge length of TDNs is increased from 7 base pairs (bp) to 36 bp. As a result, both the thermodynamics and kinetics of the interfacial DNA hybridization reaction are improved, as manifested by the increased hybridization efficiency and reduced reaction time. The sensitivity can be improved from 10 pM to 1 fM. In addition, the TDN-based biosensing interface shows excellent anti-nonspecific adsorption ability, which can effectively minimize the adsorption of nonspecific interferences in complexed matrices. Because of these superior properties of TDN-based sensors, they can be directly used for analyzing low-abundance microRNAs in real clinical samples (142). As an example, using an electrochemical TDN sensor, Wen et al. (135) detected let-7 and miR-7 microRNAs with 10 aM sensitivity, which were also applied to differentiate microRNA expression levels in tumor tissues.

The TDN-based platform provides a powerful method for protein immobilization (**Figure 6*d***). Proteins are usually immobilized on the interface via physical adsorption or covalent conjugation, which does not support proper orientation and tends to have aggregations. Hence, the activity loss is a major problem in protein assays in enzyme-linked immunosorbent assays (ELISAs), protein microarrays, and immunosensors. Our group (132) employed TDN-engineered interfaces to site specifically anchor DNA–conjugated antibodies via the DNA bridge. Based on this new strategy, we found that the sensitivity of the electrochemical immunosensors could be improved by 2–3 orders of magnitude for a range of analytes, including tumor necrosis factor-α, prostate-specific antigen, and alpha-fetoprotein.

Aptamer can also be anchored on a TDN–decorated interface for biosensing development (75, 133). Pei et al. (75) appended an aptamer on the tops of TDNs to specifically detect thrombin (**Figure 6*d***). After binding with a biotin–modified aptamer signal strand, thrombin and the aptamer pairs formed a stable sandwich structure to signal the presence of 100 pM of thrombin. Similar strategies were applied to the detection of small molecules or ions by using corresponding aptamers or DNAzymes. For example, Wen et al. (133) devised a TDN-decorated biosensor using a cocaine aptamer (**Figure 6*e***). The aptamer was split into two fragments: One was used as the capture probe and the other used with a biotin label as the signaling probe. The entanglement between aptamers at the interface was minimized due to the nanoscale distance control of TDNs. Target binding triggered the formation of an intact aptamer that brought biotin and related avidin–conjugated HRP to the electrode surface, which could sensitively detect as little as

33 nM of cocaine. This high sensitivity arises from the homogeneous distribution of TDNs on the interfaces that facilitate aptamer assembly and cocaine recognition.

## 5. IN VIVO BIOSENSING

FNAs hold great promise for intracellular and in vivo biosensing owing to their efficient cell penetration and resistance to cleavage by nucleases. The stability of probes in biological fluids is a crucial factor for in vivo biosensing detection. Wang and colleagues (143) investigated the degradation properties of double-stranded DNA (dsDNA) and TDNs in serum. They found that 20-bp dsDNA could stay stable for ~1 h in 80% mouse serum (**Figure 7*a***), whereas TDNs remain stable after incubation for 12 h. After 24 h of incubation, TDNs still exist in the serum, which demonstrates TDNs' high resistance to cleavage. Liang et al. (144) found that TDNs were intact for many hours, even in lysosomes. Interestingly, a DNA nanostructure can not only protect itself from degradation, but it can also sequester linked DNA strands and protect them from cleavage by multiple nucleases. Yan and colleagues (22) further analyzed the protection ability of DNA nanostructures on proteins (**Figure 7*a***). They encapsulated enzymes in DNA nanocages and compared the degradation of proteases on enzymes inside the nanocages and free in solution. They found that the enzymes can retain more than 95% of their initial activity in DNA nanocages after 24 h of being subjected to degradation with trypsin (22).

To detect intracellular targets, the probes have to move across the cell membrane. Our group (144) as well as that of Turberfield (145) found that TDNs could be readily internalized by mammalian cells without using transfection reagents. We further systematically investigated the transportation pathways of TDNs across the cell membrane using total internal reflection fluorescent microscopy (144) (**Figure 7*b***). We observed that TDNs were internalized through the cytomembrane primarily via the caveolin-dependent pathway. Then TDNs were transported in a microtubule-dependent manner and eventually located inside the lysosomes. We also found that when TDNs were labeled with a nuclear localization sequence, they could escape from lysosomes and enter the nuclei, suggesting that TDN-based probes can be located by subcellular organelles. By exploiting these properties, Pei et al. (146) designed a TDN-based biosensor for intracellular detection of ATP (**Figure 7*b***). An ATP aptamer was incorporated into one edge of TDN; binding of ATP triggered the conformational change of TDN, resulting in the variation of fluorescence resonance energy transfer that can be imaged under a confocal microscope.

FNA-based biosensors not only work in living cells but also in multicellular living organisms (19) (**Figure 7*c***). In a recent study (18, 19), a pH-sensitive DNA nanodevice (I-switch) was designed and applied to indicate endosomal maturation in *Caenorhabditis elegans*. After cell internalization, specific recognition of cell-surface anionic ligand-binding receptors enabled the targeting of the I-switch to scavenger cells. Similarly, a cargo-loaded DNA icosahedron was used to target scavenger cells and deliver functional substances. TDNs labeled with folate and small interfering (si)RNAs can be used to target xenograft tumors by recognizing the overexpressed folate receptor on cancerous cells. The siRNA was delivered into the cancer cells after cell internalization of TDNs to reduce the expression level of the target gene.

FNAs have also been exploited to fabricate synthetic channels to mimic biological ion channels. The highly predictable and programmable nature of DNA nanotechnology can offer great design flexibility and atomistically define the structure of FNAs. Howorka and coworkers (72) designed an open-barrel structure using seven concatenated DNA strands, which could regulate the flux of molecules across a bilayer membrane. This DNA-based nanodevice could control which cargo was transported across a bilayer and the time when this occurred. Although this study was performed

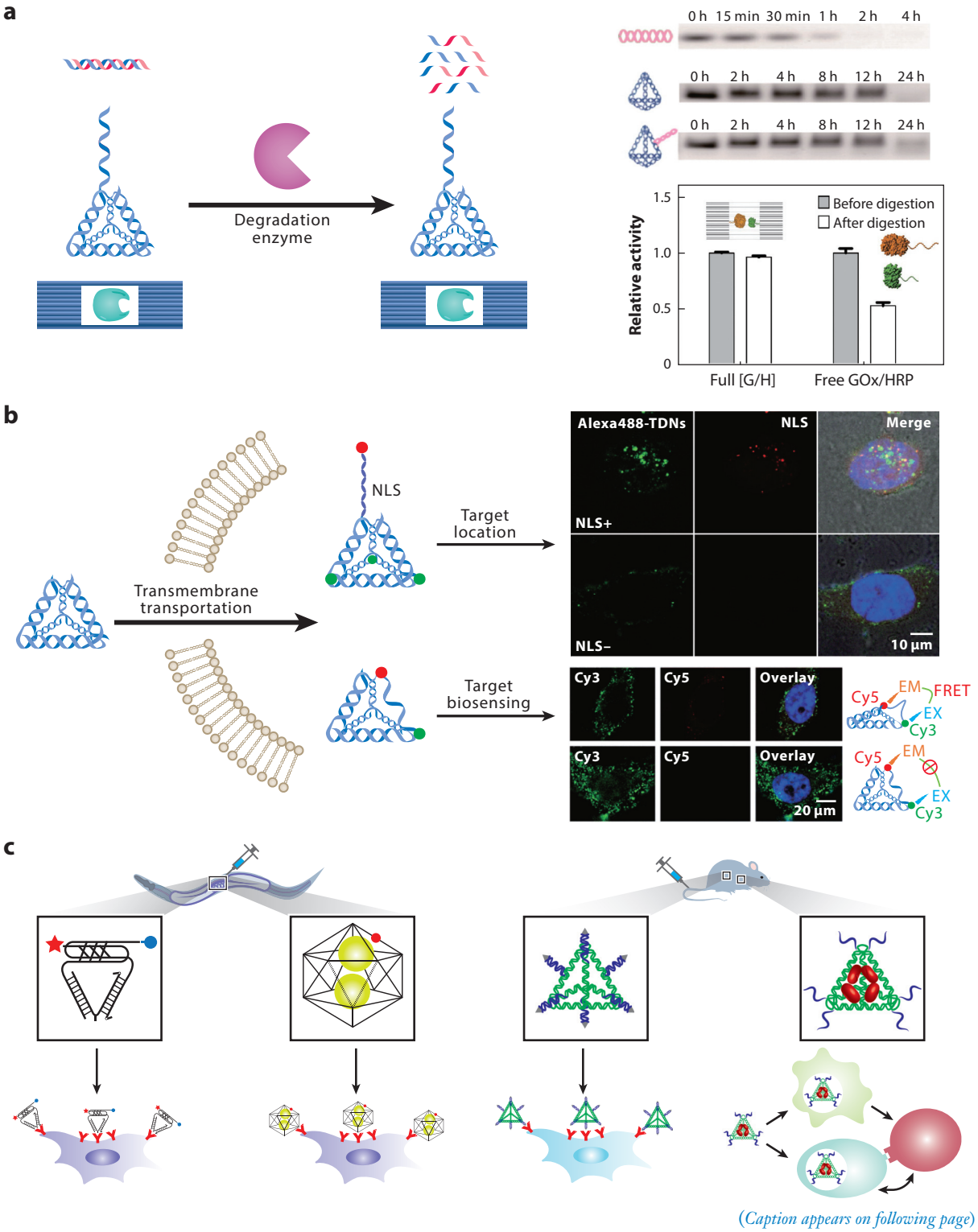


(Caption appears on following page)

**Figure 7** (*Figure appears on preceding page*)

Intracellular and in vivo biosensing using FNAs. (*a*) DNA probes encapsulated in TDNs and DNA nanocages are resistant to enzymatic cleavage. Modified with permission from Reference 143. Copyright 2016, American Chemical Society. (*b*) TDNs facilitate transmembrane transportation of biosensing probes in living cells. (*Top*) Modified with permission from Reference 144. Copyright 2014, Wiley-VCH. (*Bottom*) Modified with permission from Reference 146. Copyright 2012, Wiley-VCH. (*c*) FNAs can target specific cells in *Caenorhabditis elegans* or mice. Modified with permission from Reference 19. Copyright 2015, Nature Publishing Group. Abbreviations: Cy3/5, cyanine 3/5; EM, emission; EX, excitation; FNA, framework nucleic acid; FRET, fluorescence resonance energy transfer; GOx, glucose oxidase; HRP, horseradish peroxidase; NLS, nuclear localization sequence; TDN, tetrahedral DNA nanostructure.

in vitro, it revealed new opportunities to develop intracellular biosensors by incorporating these synthetic channels in cell membranes.

## 6. CONCLUSIONS

Advances in biosensing interfacial engineering have continued to develop over the past 20 years. The ability to immobilize biomolecules for highly controlled orientation, coupled with programmable density control capabilities, makes this interface engineering method appealing for a broad range of biosensor designs. In this review, we have summarized several important aspects of the biosensing interface, including its interfacial and biosensing applications. We highlight the use of DNA nanotechnology, especially FNAs, for engineering the biosensing interface for high-sensitivity detection of a wide range of physiologically relevant target molecules. The challenges associated with interfacial engineering remain. However, the precision of DNA nanotechnology provides a quantitative approach to probe the underlying mechanisms of biomolecular interfaces. This understanding not only increases our ability to manipulate the biosensing interface for a better biosensor, but it could be generalized to develop various biomolecular devices with electronic, optical, and acoustic output. We also expect that interfacial engineering-enabled biosensors will find new applications in quantifying biomolecules in living cells, detecting target-responsive cancer biomarkers, intelligent delivery and real-time monitoring of therapeutic agents, surveillance of infectious disease, and monitoring of environmental pollution.

## DISCLOSURE STATEMENT

The authors are not aware of any affiliations, memberships, funding, or financial holdings that might be perceived as affecting the objectivity of this review.

## ACKNOWLEDGMENTS

Part of the research discussed in this review was financially supported by the National Natural Science Foundation of China (grants 21422508, 31470960, 21390414, 21227804, 21329501), National Key R&D Program of China (grants 2016YFA0400900, 2016YFA0201200), Ministry of Science and Technology of China (grants 2013CB933802, 2013CB932803), and the Key Research Program of Frontier Sciences, Chinese Academy of Sciences (grant QYZDJ-SSW-SLH031).

## LITERATURE CITED

1. Kelley SO. 2017. Advancing ultrasensitive molecular and cellular analysis methods to speed and simplify the diagnosis of disease. *Acc. Chem. Res.* 50:503–7

2. Labib M, Sargent EH, Kelley SO. 2016. Electrochemical methods for the analysis of clinically relevant biomolecules. *Chem. Rev.* 116:9001–90
3. Lin MH, Song P, Zhou GB, Zuo XL, Aldalbahi A, et al. 2016. Electrochemical detection of nucleic acids, proteins, small molecules and cells using a DNA nanostructure-based universal biosensing platform *Nat. Protoc.* 11:1244–63
4. Kelley SO. 2017. What are clinically relevant levels of cellular and biomolecular analytes? *ACS Sens.* 2:193–97
5. Kelley SO, Mirkin CA, Walt DR, Ismagilov RF, Toner M, Sargent EH. 2014. Advancing the speed, sensitivity and accuracy of biomolecular detection using multi-length-scale engineering. *Nat. Nanotechnol.* 9:969–80
6. Fan CH, Plaxco KW, Heeger AJ. 2003. Electrochemical interrogation of conformational changes as a reagentless method for the sequence-specific detection of DNA. *PNAS* 100:9134–37
7. Sage AT, Besant JD, Lam B, Sargent EH, Kelley SO. 2014. Ultrasensitive electrochemical biomolecular detection using nanostructured microelectrodes. *Acc. Chem. Res.* 47:2417–25
8. Lu CH, Willner B, Willner I. 2013. DNA nanotechnology: from sensing and DNA machines to drug-delivery systems. *ACS Nano* 7:8320–32
9. Soleymani L, Fang ZC, Sargent EH, Kelley SO. 2009. Programming the detection limits of biosensors through controlled nanostructuring. *Nat. Nanotechnol.* 4:844–48
10. Levicky R, Horgan A. 2005. Physicochemical perspectives on DNA microarray and biosensor technologies. *Trends Biotechnol.* 23:143–49
11. Lin MH, Wang JJ, Zhou GB, Wang JB, Wu N, et al. 2015. Programmable engineering of a biosensing interface with tetrahedral DNA nanostructures for ultrasensitive DNA detection. *Angew. Chem. Int. Ed.* 54:2151–55
12. Wang SP, Cai XQ, Wang LH, Li J, Li Q, et al. 2016. DNA orientation-specific adhesion and patterning of living mammalian cells on self-assembled DNA monolayers. *Chem. Sci.* 7:2722–27
13. Ke YG, Lindsay S, Chang Y, Liu Y, Yan H. 2008. Self-assembled water-soluble nucleic acid probe tiles for label-free RNA hybridization assays. *Science* 319:180–83
14. Kilchherr F, Wachauf C, Pelz B, Rief M, Zacharias M, Dietz H. 2016. Single-molecule dissection of stacking forces in DNA. *Science* 353:aaf5508
15. Veneziano R, Ratanalert S, Zhang KM, Zhang F, Yan H, et al. 2016. Designer nanoscale DNA assemblies programmed from the top down. *Science* 352:aaf4388
16. Chen YJ, Groves B, Muscat RA, Seelig G. 2015. DNA nanotechnology from the test tube to the cell. *Nat. Nanotechnol.* 10:748–60
17. Bell NA, Keyser UF. 2016. Digitally encoded DNA nanostructures for multiplexed, single-molecule protein sensing with nanopores. *Nat. Nanotechnol.* 11:645–51
18. Modi S, Nizak C, Surana S, Halder S, Krishnan Y. 2013. Two DNA nanomachines map pH changes along intersecting endocytic pathways inside the same cell. *Nat. Nanotechnol.* 8:459–67
19. Surana S, Shenoy AR, Krishnan Y. 2015. Designing DNA nanodevices for compatibility with the immune system of higher organisms. *Nat. Nanotechnol.* 10:741–47
20. Southern E, Mir K, Shchepinov M. 1999. Molecular interactions on microarrays. *Nat. Genet.* 21:5–9
21. De Luna P Mahshid SS, Das J, Luan BQ, Sargent EH, et al. 2017. High-curvature nanostructuring enhances probe display for biomolecular detection. *Nano Lett.* 17:1289–95
22. Zhao Z, Fu JL, Dhakal S, Johnson-Buck A, Liu MH, et al. 2016. Nanocaged enzymes with enhanced catalytic activity and increased stability against protease digestion. *Nat. Commun.* 7:10619
23. Fu JL, Yang YR, Johnson-Buck A, Liu MH, Liu Y, et al. 2014. Multi-enzyme complexes on DNA scaffolds capable of substrate channelling with an artificial swinging arm. *Nat. Nanotechnol.* 9:531–36
24. Bracha D, Karzbrun E, Shemer G, Pincus PA, Bar-Ziv RH. 2013. Entropy-driven collective interactions in DNA brushes on a biochip. *PNAS* 110:4534–38
25. Gong P, Levicky R. 2008. DNA surface hybridization regimes. *PNAS* 105:5301–6
26. Opdahl A, Petrovykh DY, Kimura-Suda H, Tarlov MJ, Whitman LJ. 2007. Independent control of grafting density and conformation of single-stranded DNA brushes. *PNAS* 104:9–14
27. Hanssen BL, Siraj S, Wong DKY. 2016. Recent strategies to minimise fouling in electrochemical detection systems. *Rev. Anal. Chem.* 35. **https://doi.org/10.1515/revac-2015-0008**

28. Watkins HM, Simon AJ, Ricci F, Plaxco KW. 2014. Effects of crowding on the stability of a surface-tethered biopolymer: an experimental study of folding in a highly crowded regime. *J. Am. Chem. Soc.* 136:8923–27
29. Pei H, Zuo XL, Zhu D, Huang Q, Fan CH. 2014. Functional DNA nanostructures for theranostic applications. *Acc. Chem. Res.* 47:550–59
30. Belozerova I, Levicky R. 2012. Melting thermodynamics of reversible DNA/ligand complexes at interfaces. *J. Am. Chem. Soc.* 134:18667–76
31. Irving D, Gong P, Levicky R. 2010. DNA surface hybridization: comparison of theory and experiment. *J. Phys. Chem. B* 114:7631–40
32. Ge DB, Wang X, Williams K, Levicky R. 2012. Thermostable DNA immobilization and temperature effects on surface hybridization. *Langmuir* 28:8446–55
33. Bin XM, Sargent EH, Kelley SO. 2010. Nanostructuring of sensors determines the efficiency of biomolecular capture. *Anal. Chem.* 82:5928–31
34. Ye DK, Zuo XL, Fan CH. 2017. DNA Nanostructure-based engineering of the biosensing interface for biomolecular detection. *Prog. Chem.* 29:36–46
35. Klebe G. 2015. Applying thermodynamic profiling in lead finding and optimization. *Nat. Rev. Drug. Discov.* 14:95–110
36. Jones MR, Seeman NC, Mirkin CA. 2015. Programmable materials and the nature of the DNA bond. *Science* 347:1260901
37. Dong YC, Yang ZQ, Liu DS. 2014. DNA nanotechnology based on i-motif structures. *Acc. Chem. Res.* 47:1853–60
38. Tsukanov R, Tomov TE, Liber M, Berger Y, Nir E. 2014. Developing DNA nanotechnology using single-molecule fluorescence. *Acc. Chem. Res.* 47:1789–98
39. Chandrasekaran AR, Anderson N, Kizer M, Halvorsen K, Wang X. 2016. Beyond the fold: emerging biological applications of DNA origami. *ChemBioChem* 17:1081–89
40. Linko V, Dietz H. 2013. The enabled state of DNA nanotechnology. *Curr. Opin. Biotech.* 24:555–61
41. Zakeri B, Lu TK. 2015. DNA nanotechnology: new adventures for an old warhorse. *Curr. Opin. Chem. Biol.* 28:9–14
42. Chandrasekaran AR, Pushpanathan M, Halvorsen K. 2016. Evolution of DNA origami scaffolds. *Mater. Lett.* 170:221–24
43. Edwardson TGW, Lau KL, Bousmail D, Serpell CJ, Sleiman HF. 2016. Transfer of molecular recognition information from DNA nanostructures to gold nanoparticles. *Nat. Chem.* 8:162–70
44. Yang Y, Wang J, Shigematsu H, Xu WM, Shih WM, et al. 2016. Self-assembly of size-controlled liposomes on DNA nanotemplates. *Nat. Chem.* 8:476–83
45. Elbaz J, Cecconello A, Fan ZY, Govorov AO, Willner I. 2013. Powering the programmed nanostructure and function of gold nanoparticles with catenated DNA machines. *Nat. Commun.* 4:2000
46. Pan KY, Kim DN, Zhang F, Adendorff MR, Yan H, Bathe M. 2014. Lattice-free prediction of three-dimensional structure of programmed DNA assemblies. *Nat. Commun.* 5:5578
47. Zhang DY, Hariadi RF, Choi HMT, Winfree E. 2013. Integrating DNA strand-displacement circuitry with DNA tile self-assembly. *Nat. Commun.* 4:1965
48. Amir Y, Ben-Ishay E, Levner D, Ittah S, Abu-Horowitz A, Bachelet I. 2014. Universal computing by DNA origami robots in a living animal. *Nat. Nanotechnol.* 9:353–57
49. Cha TG, Pan J, Chen HR, Salgado J, Li X, et al. 2014. A synthetic DNA motor that transports nanoparticles along carbon nanotubes. *Nat. Nanotechnol.* 9:39–43
50. Funke JJ, Dietz H. 2015. Placing molecules with Bohr radius resolution using DNA origami. *Nat. Nanotechnol.* 11:47–52
51. Kim J, Lee J, Hamada S, Murata S, Park SH. 2015. Self-replication of DNA rings. *Nat. Nanotechnol.* 10:528–33
52. Lin CX, Yan H. 2009. DNA nanotechnology a cascade of activity. *Nat. Nanotechnol.* 4:211–12
53. Tian Y, Wang T, Liu WY, Xin HL, Li HL, et al. 2015. Prescribed nanoparticle cluster architectures and low-dimensional arrays built using octahedral DNA origami frames. *Nat. Nanotechnol.* 10:637–44
54. Udomprasert A, Bongiovanni MN, Sha RJ, Sherman WB, Wang T, et al. 2014. Amyloid fibrils nucleated and organized by DNA origami constructions. *Nat. Nanotechnol.* 9:537–41

55. Zhang F, Jiang SX, Wu SY, Li YL, Mao CD, et al. 2015. Complex wireframe DNA origami nanostructures with multi-arm junction vertices. *Nat. Nanotechnol.* 10:779–84
56. Benson E, Mohammed A, Gardell J, Masich S, Czeizler E, et al. 2015. DNA rendering of polyhedral meshes at the nanoscale. *Nature* 523:441–45
57. He Y, Ye T, Su M, Zhang C, Ribbe AE, et al. 2008. Hierarchical self-assembly of DNA into symmetric supramolecular polyhedra. *Nature* 452:198–202
58. Wei B, Dai MJ, Yin P. 2012. Complex shapes self-assembled from single-stranded DNA tiles. *Nature* 485:623–26
59. Iinuma R, Ke YG, Jungmann R, Schlichthaerle T, Woehrstein JB, Yin P. 2014. Polyhedra Self-assembled from DNA tripods and characterized with 3D DNA-PAINT. *Science* 344:65–69
60. Rogers WB, Manoharan VN. 2015. Programming colloidal phase transitions with DNA strand displacement. *Science* 347:639–42
61. Song J, Li Z, Wang PF, Meyer T, Mao CD, Ke YG. 2017. Reconfiguration of DNA molecular arrays driven by information relay. *Science* 357:aan3377
62. Sun W, Boulais E, Hakobyan Y, Wang WL, Guan A, et al. 2014. Casting inorganic structures with DNA molds. *Science* 346:1258361
63. Chao J, Liu HJ, Su S, Wang LH, Huang W, Fan CH. 2014. Structural DNA nanotechnology for intelligent drug delivery. *Small* 10:4626–35
64. Zhang F, Nangreave J, Liu Y, Yan H. 2014. Structural DNA nanotechnology: state of the art and future perspective. *J. Am. Chem. Soc.* 136:11198–211
65. Lim XZ. 2017. The architecture of structured DNA. *Nature* 546:687–89
66. Qian L, Wang Y, Zhang Z, Zhao J, Pan D, et al. 2006. Analogic China map constructed by DNA. *Chinese Sci. Bull.* 51:2973–76
67. Zhang Z, Zeng DD, Ma HW, Feng GY, Hu J, et al. 2010. A DNA-origami chip platform for label-free SNP genotyping using toehold-mediated strand displacement. *Small* 6:1854–58
68. Marras AE, Zhou LF, Su HJ, Castro CE. 2015. Programmable motion of DNA origami mechanisms. *PNAS* 112:713–18
69. Wollman AJM, Sanchez-Cano C, Carstairs HMJ, Cross RA, Turberfield AJ. 2014. Transport and self-organization across different length scales powered by motor proteins and programmed by DNA. *Nat. Nanotechnol.* 9:44–47
70. Kuzyk A, Schreiber R, Zhang H, Govorov AO, Liedl T, Liu N. 2014. Reconfigurable 3D plasmonic metamolecules. *Nat. Mater.* 13:862–66
71. Elsner M. 2013. Membrane channels built from DNA. *Nat. Biotechnol.* 31:125–25
72. Burns JR, Seifert A, Fertig N, Howorka S. 2016. A biomimetic DNA-based channel for the ligand-controlled transport of charged molecular cargo across a biological membrane. *Nat. Nanotechnol.* 11:152–56
73. Hao CH, Li X, Tian C, Jiang W, Wang GS, Mao CD. 2014. Construction of RNA nanocages by re-engineering the packaging RNA of Phi29 bacteriophage. *Nat. Commun.* 5:3890
74. Geary C, Rothemund PWK, Andersen ES. 2014. A single-stranded architecture for cotranscriptional folding of RNA nanostructures. *Science* 345:799–804
75. Pei H, Lu N, Wen YL, Song SP, Liu Y, et al. 2010. A DNA nanostructure-based biomolecular probe carrier platform for electrochemical biosensing. *Adv. Mater.* 22:4754–58
76. Zhu D, Pei H, Yao GB, Wang LH, Su S, et al. 2016. A surface-confined proton-driven DNA pump using a dynamic 3D DNA Scaffold. *Adv. Mater.* 28:6860–65
77. Vainrub A, Pettitt BM. 2003. Sensitive quantitative nucleic acid detection using oligonucleotide microarrays. *J. Am. Chem. Soc.* 125:7798–99
78. Hagan MF, Chakraborty AK. 2004. Hybridization dynamics of surface immobilized DNA. *J. Chem. Phys.* 120:4958–68
79. Herne TM, Tarlov MJ. 1997. Characterization of DNA probes immobilized on gold surfaces. *J. Am. Chem. Soc.* 119:8916–20
80. Levicky R, Herne TM, Tarlov MJ, Satija SK. 1998. Using self-assembly to control the structure of DNA monolayers on gold: a neutron reflectivity study. *J. Am. Chem. Soc.* 120:9787–92

81. Petrovykh DY, Kimura-Suda H, Whitman LJ, Tarlov MJ. 2003. Quantitative analysis and characterization of DNA immobilized on gold. *J. Am. Chem. Soc.* 125:5219–26
82. Petrovykh DY, Perez-Dieste V, Opdahl A, Kimura-Suda H, Sullivan JM, et al. 2006. Nucleobase orientation and ordering in films of single-stranded DNA on gold. *J. Am. Chem. Soc.* 128:2–3
83. Gillen G, Bennett J, Tarlov MJ, Burgess F. 1994. Molecular imaging secondary-ion mass-spectrometry for the characterization of patterned self-assembled monolayers on silver and gold. *Anal. Chem.* 66:2170–74
84. Arinaga K, Rant U, Tornow M, Fujita S, Abstreiter G, Yokoyama N. 2006. The role of surface charging during the coadsorption of mercaptohexanol to DNA layers on gold: direct observation of desorption and layer reorientation. *Langmuir* 22:5560–62
85. Park S, Brown KA, Hamad-Schifferli K. 2004. Changes in oligonucleotide conformation on nanoparticle surfaces by modification with mercaptohexanol. *Nano Lett.* 4:1925–29
86. Henry OYF, Perez JG, Sanchez JLA, O'Sullivan CK. 2010. Electrochemcial characterisation and hybridisation efficiency of co-assembled monolayers of PEGylated ssDNA and mercaptohexanol on planar gold electrodes. *Biosens. Bioelectron.* 25:978–83
87. Zhang LL, Li ZG, Zhou XP, Yang GZ, Yang JM, et al. 2015. Hybridization performance of DNA/mercaptohexanol mixed monolayers on electrodeposited nanoAu and rough Au surfaces. *J. Electroanal. Chem.* 757:203–9
88. Zhang J, Song SP, Zhang LY, Wang LH, Wu HP, et al. 2006. Sequence-specific detection of femtomolar DNA via a chronocoulometric DNA sensor (CDS): effects of nanoparticle-mediated amplification and nanoscale control of DNA assembly at electrodes. *J. Am. Chem. Soc.* 128:8575–80
89. Asav E, Sagiroglu A, Sezginturk MK. 2016. Quantitative analysis of a promising cancer biomarker, calretinin, by a biosensing system based on simple and effective immobilization process. *Electroanalysis* 28:334–42
90. Zhang J, Lao RJ, Song SP, Yan ZY, Fan CH. 2008. Design of an oligonucleotide-incorporated nonfouling surface and its application in electrochemical DNA sensors for highly sensitive and sequence-specific detection of target DNA. *Anal. Chem.* 80:9029–33
91. Wu J, Campuzano S, Halford C, Haake DA, Wang J. 2010. Ternary surface monolayers for ultrasensitive (zeptomole) amperometric detection of nucleic acid hybridization without signal amplification. *Anal. Chem.* 82:8830–37
92. Li Y, Zhao M, Wang H. 2017. Label-free peptide aptamer based impedimetric biosensor for highly sensitive detection of TNT with a ternary assembly layer. *Anal. Bioanal. Chem.* 409:6371–77
93. Dharuman V, Vijayaraj K, Radhakrishnan S, Dinakaran T, Narayanan JS, et al. 2011. Sensitive label-free electrochemical DNA hybridization detection in the presence of 11-mercaptoundecanoic acid on the thiolated single strand DNA and mercaptohexanol binary mixed monolayer surface. *Electrochim. Acta* 56:8147–55
94. Kimura-Suda H, Petrovykh DY, Tarlov MJ, Whitman LJ. 2003. Base-dependent competitive adsorption of single-stranded DNA on gold. *J. Am. Chem. Soc.* 125:9014–15
95. Demers LM, Ostblom M, Zhang H, Jang NH, Liedberg B, Mirkin CA. 2002. Thermal desorption behavior and binding properties of DNA bases and nucleosides on gold. *J. Am. Chem. Soc.* 124:11248–49
96. Storhofff JJ, Elghanian R, Mirkin CA, Letsinger RL. 2002. Sequence-dependent stability of DNA-modified gold nanoparticles. *Langmuir* 18:6666–70
97. Schreiner SM, Shudy DF, Hatch AL, Opdahl A, Whitman LJ, Petrovykh DY. 2010. Controlled and efficient hybridization achieved with DNA probes immobilized solely through preferential DNA-substrate interactions. *Anal. Chem.* 82:2803–10
98. Liu P, Wang DD, Zhou YL, Wang HY, Yin HS, Ai SY. 2016. DNA methyltransferase detection based on digestion triggering the combination of poly adenine DNA with gold nanoparticles. *Biosens. Bioelectron.* 80:74–78
99. Pei H, Li F, Wan Y, Wei M, Liu HJ, et al. 2012. Designed diblock oligonucleotide for the synthesis of spatially isolated and highly hybridizable functionalization of DNA-gold nanoparticle nanoconjugates. *J. Am. Chem. Soc.* 134:11876–79
100. Zhu D, Song P, Shen JW, Su S, Chao J, et al. 2016. PolyA-mediated DNA assembly on gold nanoparticles for thermodynamically favorable and rapid hybridization analysis. *Anal. Chem.* 88:4949–54

101. Guo JX, Chen YL, Jiang YJ, Ju HX. 2017. Polyadenine-modulated DNA conformation monitored by surface-enhanced Raman scattering (SERS) on multibranched gold nanoparticles and its sensing application. *Chem. Eur. J.* 23:9332–37
102. Zhu D, Pei H, Chao J, Su S, Aldalbahi A, et al. 2015. Poly-adenine-based programmable engineering of gold nanoparticles for highly regulated spherical DNAzymes. *Nanoscale* 7:18671–76
103. Wen JL, Chen JH, Zhuang L, Zhou SG. 2016. Designed diblock hairpin probes for the nonenzymatic and label-free detection of nucleic acid. *Biosens. Bioelectron.* 79:656–60
104. Zhu D, Chao J, Pei H, Zuo XL, Huang Q, et al. 2015. Coordination-mediated programmable assembly of unmodified oligonucleotides on plasmonic silver nanoparticles. *ACS Appl. Mater. Interfaces* 7:11047–52
105. Lu C, Huang ZC, Liu BW, Liu YB, Ying YB, Liu JW. 2017. Poly-cytosine DNA as a high-affinity ligand for inorganic nanomaterials. *Angew. Chem. Int. Ed.* 56:6208–12
106. Fang ZC, Soleymani L, Pampalakis G, Yoshimoto M, Squire JA, et al. 2009. Direct profiling of cancer biomarkers in tumor tissue using a multiplexed nanostructured microelectrode integrated circuit. *ACS Nano* 3:3207–13
107. Soleymani L, Fang ZC, Lam B, Bin XM, Vasilyeva E, et al. 2011. Hierarchical nanotextured microelectrodes overcome the molecular transport barrier to achieve rapid, direct bacterial detection. *ACS Nano* 5:3360–66
108. Das J, Kelley SO. 2011. Protein detection using arrayed microsensor chips: tuning sensor footprint to achieve ultrasensitive readout of CA-125 in serum and whole blood. *Anal. Chem.* 83:1167–72
109. Das J, Kelley SO. 2013. Tuning the bacterial detection sensitivity of nanostructured microelectrodes. *Anal. Chem.* 85:7333–38
110. Ivanov I, Stojcic J, Stanimirovic A, Sargent E, Nam RK, Kelley SO. 2013. Chip-based nanostructured sensors enable accurate identification and classification of circulating tumor cells in prostate cancer patient blood samples. *Anal. Chem.* 85:398–403
111. Lam B, Fang ZC, Sargent EH, Kelley SO. 2012. Polymerase chain reaction-free, sample-to-answer bacterial detection in 30 minutes with integrated cell lysis. *Anal. Chem.* 84:21–25
112. Smith SJ, Nemr CR, Kelley SO. 2017. Chemistry-driven approaches for ultrasensitive nucleic acid detection. *J. Am. Chem. Soc.* 139:1020–28
113. Das J, Ivanov I, Montermini L, Rak J, Sargent EH, Kelley SO. 2015. An electrochemical clamp assay for direct, rapid analysis of circulating nucleic acids in serum. *Nat. Chem.* 7:569–75
114. Besant JD, Das J, Burgess IB, Liu WH, Sargent EH, Kelley SO. 2015. Ultrasensitive visual read-out of nucleic acids using electrocatalytic fluid displacement. *Nat. Commun.* 6:6978
115. Lam B, Das J, Holmes RD, Live L, Sage A, et al. 2013. Solution-based circuits enable rapid and multiplexed pathogen detection. *Nat. Commun.* 4:2001
116. Sage AT, Besant JD, Mahmoudian L, Poudineh M, Bai X, et al. 2015. Fractal circuit sensors enable rapid quantification of biomarkers for donor lung assessment for transplantation. *Sci. Adv.* 1:e1500417
117. Condon A. 2006. Designed DNA molecules: principles and applications of molecular nanotechnology. *Nat. Rev. Genet.* 7:565–75
118. Gopinath A, Rothemund PWK. 2014. Optimized assembly and covalent coupling of single-molecule DNA origami nano arrays. *ACS Nano* 8:12030–40
119. Acuna GP, Bucher M, Stein IH, Steinhauer C, Kuzyk A, et al. 2012. Distance dependence of single-fluorophore quenching by gold nanoparticles studied on DNA origami. *ACS Nano* 6:3189–95
120. Howorka S. 2016. Changing of the guard. *Science* 352:890–91
121. Shen WQ, Bruist MF, Goodman SD, Seeman NC. 2004. A protein-driven DNA device that measures the excess binding energy of proteins that distort DNA. *Angew. Chem. Int. Ed.* 43:4750–52
122. Tintore M, Gallego I, Manning B, Eritja R, Fabrega C. 2013. DNA origami as a DNA repair nanosensor at the single-molecule level. *Angew. Chem. Int. Ed.* 52:7747–50
123. Wang DF, Fu YM, Yan J, Zhao B, Dai B, et al. 2014. Molecular logic gates on DNA origami nanostructures for microRNA diagnostics. *Anal. Chem.* 86:1932–36
124. Chhabra R, Sharma J, Ke Y, Liu Y, Rinker S, et al. 2007. Spatially addressable multiprotein nanoarrays templated by aptamer-tagged DNA nanoarchitectures. *J. Am. Chem. Soc.* 129:10304–5
125. Numajiri K, Yamazaki T, Kimura M, Kuzuya A, Komiyama M. 2010. Discrete and active enzyme nanoarrays on DNA origami scaffolds purified by affinity tag separation. *J. Am. Chem. Soc.* 132:9937–39

126. Wilner OI, Weizmann Y, Gill R, Lioubashevski O, Freeman R, Willner I. 2009. Enzyme cascades activated on topologically programmed DNA scaffolds. *Nat. Nanotechnol.* 4:249–54
127. Fu YM, Zeng DD, Chao J, Jin YQ, Zhang Z, et al. 2013. Single-step rapid assembly of DNA Origami nanostructures for addressable nanoscale bioreactors. *J. Am. Chem. Soc.* 135:696–702
128. Li YL, Liu ZY, Yu GM, Jiang W, Mao CD. 2015. Self-assembly of molecule-like nanoparticle clusters directed by DNA nanocages. *J. Am. Chem. Soc.* 137:4320–23
129. Pilo-Pais M, Watson A, Demers S, LaBean TH, Finkelstein G. 2014. Surface-enhanced Raman scattering plasmonic enhancement using DNA origami-based complex metallic nanostructures. *Nano Lett.* 14:2099–104
130. Pal S, Deng ZT, Wang HN, Zou SL, Liu Y, Yan H. 2011. DNA directed self-assembly of anisotropic plasmonic nanostructures. *J. Am. Chem. Soc.* 133:17606–09
131. Subramanian HKK, Chakraborty B, Sha R, Seeman NC. 2011. The label-free unambiguous detection and symbolic display of single nucleotide polymorphisms on DNA origami. *Nano Lett.* 11:910–13
132. Chen XQ, Zhou GB, Song P, Wang JJ, Gao JM, et al. 2014. Ultrasensitive electrochemical detection of prostate-specific antigen by using antibodies anchored on a DNA nanostructural scaffold. *Anal. Chem.* 86:7337–42
133. Wen YL, Pei H, Wan Y, Su Y, Huang Q, et al. 2011. DNA nanostructure-decorated surfaces for enhanced aptamer-target binding and electrochemical cocaine sensors. *Anal. Chem.* 83:7418–23
134. Liu G, Wan Y, Gau V, Zhang J, Wang LH, et al. 2008. An enzyme-based E-DNA sensor for sequence-specific detection of femtomolar DNA targets. *J. Am. Chem. Soc.* 130:6820–25
135. Wen YL, Pei H, Shen Y, Xi JJ, Lin MH, et al. 2012. DNA Nanostructure-based interfacial engineering for PCR-free ultrasensitive electrochemical analysis of microRNA. *Sci. Rep.* 2:867
136. Xiao Y, Lou XH, Uzawa T, Plakos KJI, Plaxco KW, Soh HT. 2009. An electrochemical sensor for single nucleotide polymorphism detection in serum based on a triple-stem DNA probe. *J. Am. Chem. Soc.* 131:15311–16
137. Xiao Y, Qu XG, Plaxco KW, Heeger AJ. 2007. Label-free electrochemical detection of DNA in blood serum via target-induced resolution of an electrode-bound DNA pseudoknot. *J. Am. Chem. Soc.* 129:11896–97
138. Xiao Y, Lai RY, Plaxco KW. 2007. Preparation of electrode-immobilized, redox-modified oligonucleotides for electrochemical DNA and aptamer-based sensing. *Nat. Protoc.* 2:2875–80
139. Lai RY, Lagally ET, Lee SH, Soh HT, Plaxco KW, Heeger AJ. 2006. Rapid, sequence-specific detection of unpurified PCR amplicons via a reusable, electrochemical sensor. *PNAS* 103:4017–21
140. Xiao Y, Lubin AA, Baker BR, Plaxco KW, Heeger AJ. 2006. Single-step electronic detection of femtomolar DNA by target-induced strand displacement in an electrode-bound duplex. *PNAS* 103:16677–80
141. Lu N, Pei H, Ge ZL, Simmons CR, Yan H, Fan CH. 2012. Charge transport within a three-dimensional DNA nanostructure framework. *J. Am. Chem. Soc.* 134:13148–51
142. Ge ZL, Lin MH, Wang P, Pei H, Yan J, et al. 2014. Hybridization chain reaction amplification of microRNA detection with a tetrahedral DNA nanostructure-based electrochemical biosensor. *Anal. Chem.* 86:2124–30
143. Jiang DW, Sun YH, Li J, Li Q, Lv M, et al. 2016. Multiple-armed tetrahedral DNA nanostructures for tumor-targeting, dual-modality in vivo imaging. *ACS Appl. Mater. Interfaces* 8:4378–84
144. Liang L, Li J, Li Q, Huang Q, Shi JY, et al. 2014. Single-particle tracking and modulation of cell entry pathways of a tetrahedral DNA nanostructure in live cells. *Angew. Chem. Int. Ed.* 53:7745–50
145. Walsh AS, Yin HF, Erben CM, Wood MJA, Turberfield AJ. 2011. DNA cage delivery to mammalian cells. *ACS Nano* 5:5427–32
146. Pei H, Liang L, Yao GB, Li J, Huang Q, Fan CH. 2012. Reconfigurable three-dimensional DNA nanostructures for the construction of intracellular logic sensors. *Angew. Chem. Int. Ed.* 51:9020–24